

Real-Time Monitoring and Quantifying 3D Tumor Spheroid Invasion Using the Agilent xCELLigence RTCA eSight System

Author

Grace Yang, Tian Wang, Peifang Ye,
Xiaoyu Zhang, Ryan Raver,
Agilent Technologies, Inc.

Abstract

The study of cell invasion is of great significance to cancer research, because 90% of the deaths of cancer patients are related to cancer metastasis, and the invasion and infiltration of cancer cells into surrounding tissues and chambers is an essential step of cancer metastasis. As a result, accurate and reliable methods for evaluating cell invasion are very useful for understanding pathophysiological activities including cancer metastasis and inflammatory diseases. As 3D spheroid models preserve the physiological and physical gradient inside the tumor more effectively, the invasion of 3D model systems can simulate the invasion of tumor cells into the surrounding cell matrix and tissues more accurately. In this technical overview, we embedded a single HT-1080 tumor spheroid into extracellular matrix, using the 3D spheroid invasion module of the Agilent xCELLigence RTCA eSight system to continuously acquire brightfield and fluorescent channel images during the invasion process according to a preset procedure. Combined with refined image processing and continuous monitoring, we achieved precise quantification of the invasiveness of HT-1080 tumor spheroids.

Introduction

Tumor metastasis is an important hallmark of malignancy and accounts for 90% of cancer-related deaths in patients with palpable clinical traits.² To metastasize, cancer cells must escape from the primary tumor, form invadopodia to degrade the extracellular matrix (ECM), invade local tissues and cavities, and then enter circulation to spread further.²⁻⁵ Therefore, the ability of tumor cells to invade is related to their metastatic potential, and intervention in tumor invasion is expected to help improve the clinical prognosis of tumor patients. To have a better and more in-depth understanding of the pathophysiological activities involved in metastatic cancer, accurate and reliable methods for evaluating cell invasion are greatly needed. Various methods have been developed to analyze and quantify cell migration and invasion capacity, such as scratching a single layer of tumor cells plated on a 2D plate to heal (2D wound healing assay) or embedding a single tumor within a 3D ECM (3D invasion assay). In vitro 3D spheroids can better mimic the behavior of cells that grow in vivo.⁶ Therefore, the invasion of 3D spheroids can provide more reliable data to study the metastasizing potential of tumor cells. This includes examining the morphological changes of various cell lines during invasion, as well as the strength of their invasion ability. Furthermore, 3D invasion assays help to better comprehend how cell lines react to different chemo-inhibitors of metastasis.

Here, we used and optimized protocol for a simple and commonly used model of 3D tumor invasion assay, consisting of a single tumor spheroid embedded within an ECM.⁷ We combined this model with an automated image acquisition and analysis system, the Agilent xCELLigence RTCA eSight, to monitor and quantify compound-treated 3D tumor spheroid invasion in Matrigel in real-time with brightfield and fluorescent imaging. Specifically, compound-containing Matrigel was laid onto tumor spheroids and compound-containing medium was added to the Matrigel after polymerization. After image processing, the eSight software quantifies the spheroid invasion and evaluates the efficacy of the compound by tracking and calculating the area of invadopodia protruding from the spheroid. The xCELLigence RTCA eSight provides a unique real-time live-cell imaging capability along with automatic quantification of 3D tumor spheroid invasive protrusions, which enables potential advancement of new preclinical treatments and serves as an in vitro platform for antitumor drug screening.

Materials and methods

Cells and reagents

Cell maintenance and assays were conducted at 37 °C in a 5% CO₂ incubator. Cell lines used and their growth media are shown in Table 1. FBS was from Gibco (part number 10099-141) and Pen/Strep was from HyClone (part number SV30010).

Table 1. Cell lines and medium.

Cell Lines	Base Medium	Medium Supplements
HT-1080	EMEM (ATCC, p/n 30-2003)	10% FBS + 1% pen/strep
U-87	50% F12 (Gibco, p/n 11765-054) + 50% MEM (Gibco, p/n 11095-080)	10% FBS + 1% pen/strep
SKOV3	McCoy's 5A (Gibco, p/n 16600-082)	10% FBS + 1% pen/strep
BT474	Hybri-Care (ATCC, p/n 46-X)	10% FBS + 1% pen/strep

1. HT-1080 Red cells, which express a nuclear-localized red fluorescent protein (RFP), were produced by transducing the parental cells with the Agilent eLenti Red reagent (part number 8711011).
2. 72 hours after transduction, cells were shifted in a complete growth medium containing 2 µg/mL puromycin for an additional 14 days to select for transduced cells.
3. Cell lines were seeded into 96-well ultralow attachment (ULA) plate (Corning, part number 7007) at a density of 2,500 cells/well in 150 µL media separately. The ULA plate was then centrifuged (125 g, 10 minutes) at room temperature to settle down the cells quickly. Three days after cell seeding, cells grew into tumor spheroids.
4. 120 µL of medium was gently removed from each well, avoiding contact with the spheroids.

Matrigel

5. To avoid premature gelation of Matrigel, the plate containing the spheroid was chilled on ice and ensured that all subsequent Matrigel-related operations were carried out on the ice and all containers or tips were prechilled.
6. Following this, 50 µL of 8 mg/mL Matrigel was gently laid on top of the spheroids. Note: It is important to keep the tips vertical up the spheroids when adding the Matrigel, and to dispense slowly to avoid disturbing the spheroids.

3D tumor invasion assay

During this process, if the tumor spheroid is shifted from the center of the wells due to operation, centrifuging the plate (4 °C, 300 g, 5 minutes) could help the spheroid back to the well center.

7. The plate was transferred to a 37 °C/5% CO₂ incubator and incubated for one hour to solidify the Matrigel.
8. 100 µL complete growth medium was added to the top of the Matrigel.
9. The experiment was set as follows and proceeded to real-time monitoring:
 - a. Assay Type: 3D Spheroids Invasion
 - b. 10x objective, stitch, 2 x 2 images/well (or 5x objective, 96-well plate, 1 image/well)
 - c. Channel selection: Brightfield + Red (Exposure time: 15 ms) (Red, Green, and Blue fluorescence channels can be used together when necessary)
 - d. Scan interval: Every four hours for up to eight days

For the invasion inhibition assay induced by drug treatment, both Matrigel and subsequently added media contained 1x compound (Cytochalasin D, Thermo Fisher Scientific, part number PHZ1063, or Ilomastat, GM6001, MedChemExpress, part number HY-15768, or DMSO control). Figure 1 shows a brief workflow.

Key parameters used for the 3D spheroid invasion assay

The reliability of the three-dimensional in vitro tumor spheroid invasion model for assessing the inhibitory effect of metastasis depends on its ability to identify the spheroid invasion area. In this application, the invading cell area was defined as the total area of the spheroid at time **t** (following treatment) subtracting the total area of the spheroid at time **t₀** (initial area, the area right after the addition of Matrigel and compound).⁷ The equation **Invading cell area = Area_t – Area_{t₀}** was designed to allow for the rapid quantitation of invasion out of a large number of spheroids. Additionally, the invading ratio (ratio of the invading area to the initial area of the spheroid) was calculated as: **Invading ratio = (Area_t – Area_{t₀})/(Area_{t₀})**.

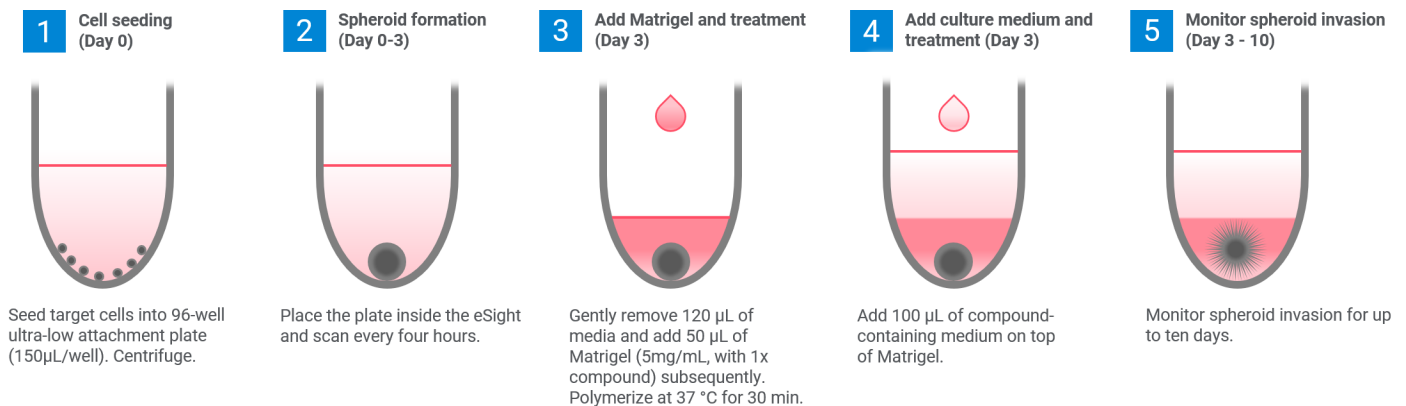


Figure 1. Brief workflow for the 3D spheroid invasion assay using the Agilent xCELLigence RTCA eSight system from days 0 to 10.

Results and discussion

Various invasive abilities of different cell lines

Invadopodia are finger-like, actin-rich protrusions that are required for metastatic tumor cells to degrade the ECM to metastasis. To evaluate the metastatic potential of tumor cells, HT-1080, U-87, SKOV3, and BT474 spheroids were formed for 72 hours in a ULA round-bottom 96-well plate and subsequently embedded in Matrigel (5 mg/mL). Changes in tumor spheroid invasive properties were kinetically monitored over time (five days).

As shown in Figure 2, the tumor cell invasion processes, including details of the invadopodia extending into the matrigel are captured clearly and unambiguously by the 3D spheroid invasion module of the eSight system. The ability of different cell lines to invade was varied. This assay showed that cell lines HT-1080 and U-87, whose invasion commenced directly after implantation into the matrix, have been found to display radial invasion areas and are classified as strongly invasive, while SKOV3 shows weak invasiveness. BT474 did not invade.

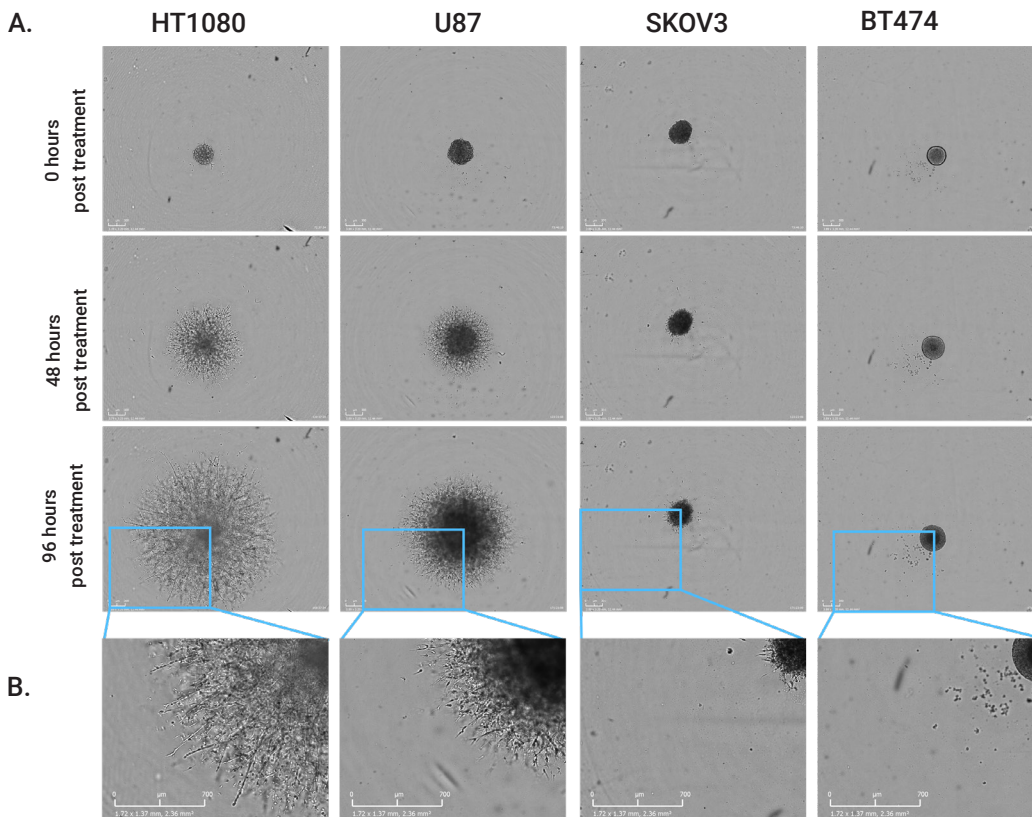


Figure 2. Representative images show the invasion abilities of various tumor spheroid cell lines. (A) The HT-1080, U-87, and SKOV3 cells show invasion from the spheroids, whereas the BT474 cells do not. The invasion of HT-1080 cells is most pronounced after 96 hours. The scale bar represents 300 μm . (B) Enlargement of a section of the spheroids to show the details of the invadopodia extending into the Matrigel for each of the cell lines. The magnification showed the invadopodia morphology of HT-1080 and U-87 tumor spheroids was similar, whereas SKOV3 and BT474 showed weak invasion or no invasion.

Dose-dependent inhibition of the 3D HT-1080 spheroid invasion by Cytochalasin D

Cytochalasin D is a cell-permeable fungal toxin that disrupts actin filaments and inhibits actin polymerization. In this way, Cytochalasin D can interfere with a variety of processes, including cell movement (such as migration and invasion), growth, phagocytosis, threshing, and secretion. To validate this analysis approach, we explored the HT-1080 tumor spheroid invasion inhibition effect of different concentrations of cytochalasin D. As shown in Figure 3 , the invading cell area

and the invading ratio (ratio of invading cell area to the initial spheroid area) were calculated and plotted in Figures 3B and 3C. Both metrics, the invading cell area and the invading ratio, are useful in quantifying the cell invasiveness. Figure 3 illustrates that the higher the cytochalasin D concentration, the stronger the inhibitory effect on HT-1080 spheroid invasion, as shown by a decrease in cell invading area and the invading ratio.

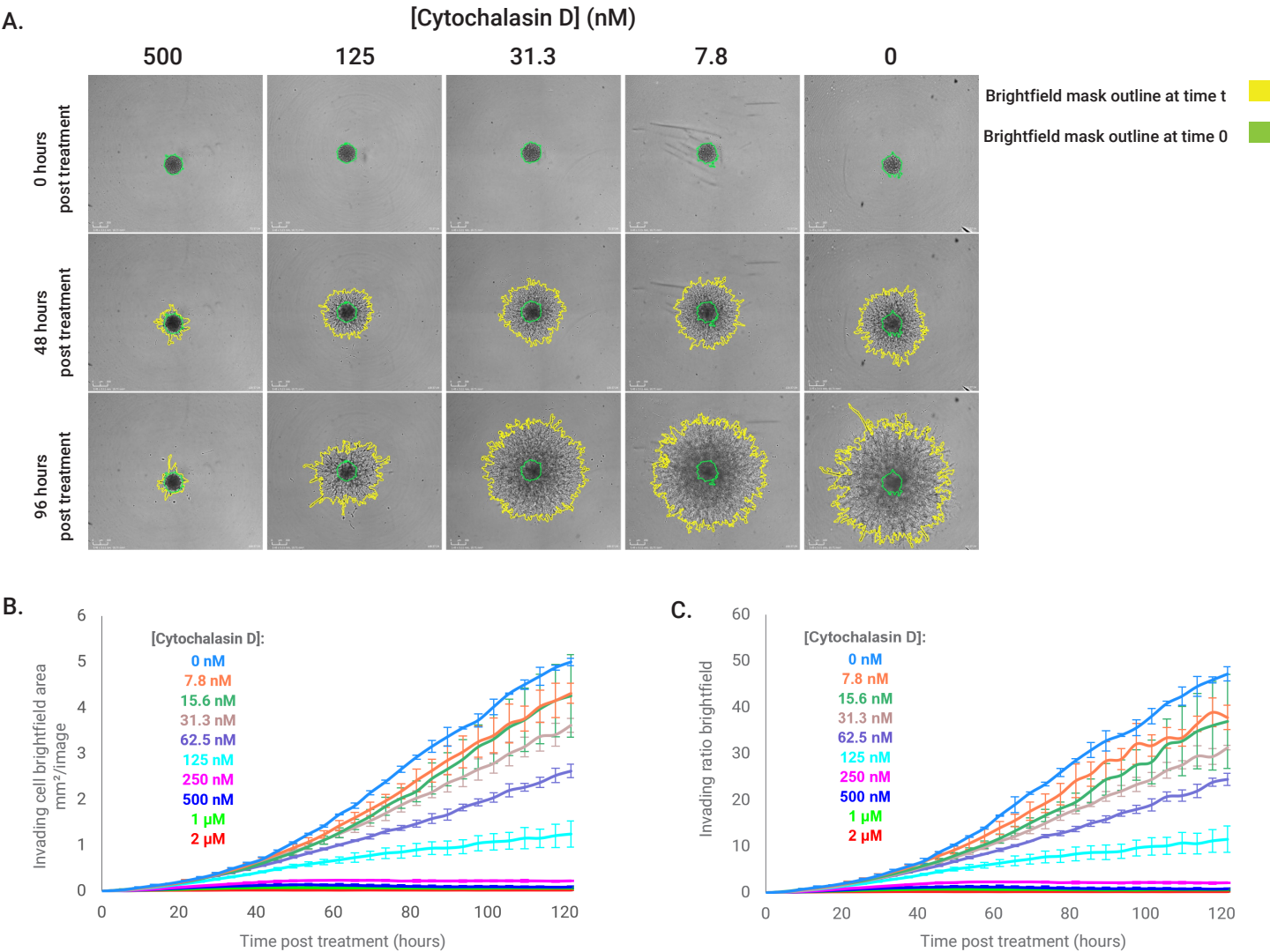


Figure 3. Cytochalasin D dose-dependently inhibits HT-1080 spheroid invasion through brightfield recognition. (A) Images show HT-1080 spheroids at 0, 48, and 96 hours after treatment with different concentrations of cytochalasin D. The whole spheroids with cells invading into Matrigel were recognized by Agilent eSight software and outlined in yellow. For comparison, the spheroid outline at time zero (right after Matrigel and compound addition) is shown in green. The impacts of cytochalasin D on the cell invasion progress were quantified by invading cell brightfield area (B) and invading ratio brightfield (C) as a function of time.

For some applications, multiple cell types, such as various nonmalignant cells, may be used in the 3D spheroid formation. To better monitor tumor cell invasion, fluorescence labeled tumor cells will be more suitable for tracking their invasion process. Here, we also showcase that fluorescent images of the invasion can be precisely quantified by the software. The invading cell area and the invading ratio based on red fluorescence were plotted over time, shown in Figure 4.

Using the brightfield and red image-based readouts, the IC₅₀ values for cytochalasin D inhibiting spheroid invasion were calculated, respectively. The areas under the curve, spanning from the time of drug addition to 120 hours post drug addition, were plotted as a function of cytochalasin D concentration to yield the dose-response curves seen in Figure 5A . The IC₅₀ values are similar, which demonstrates the accuracy of invasion quantification without fluorescent labeling.

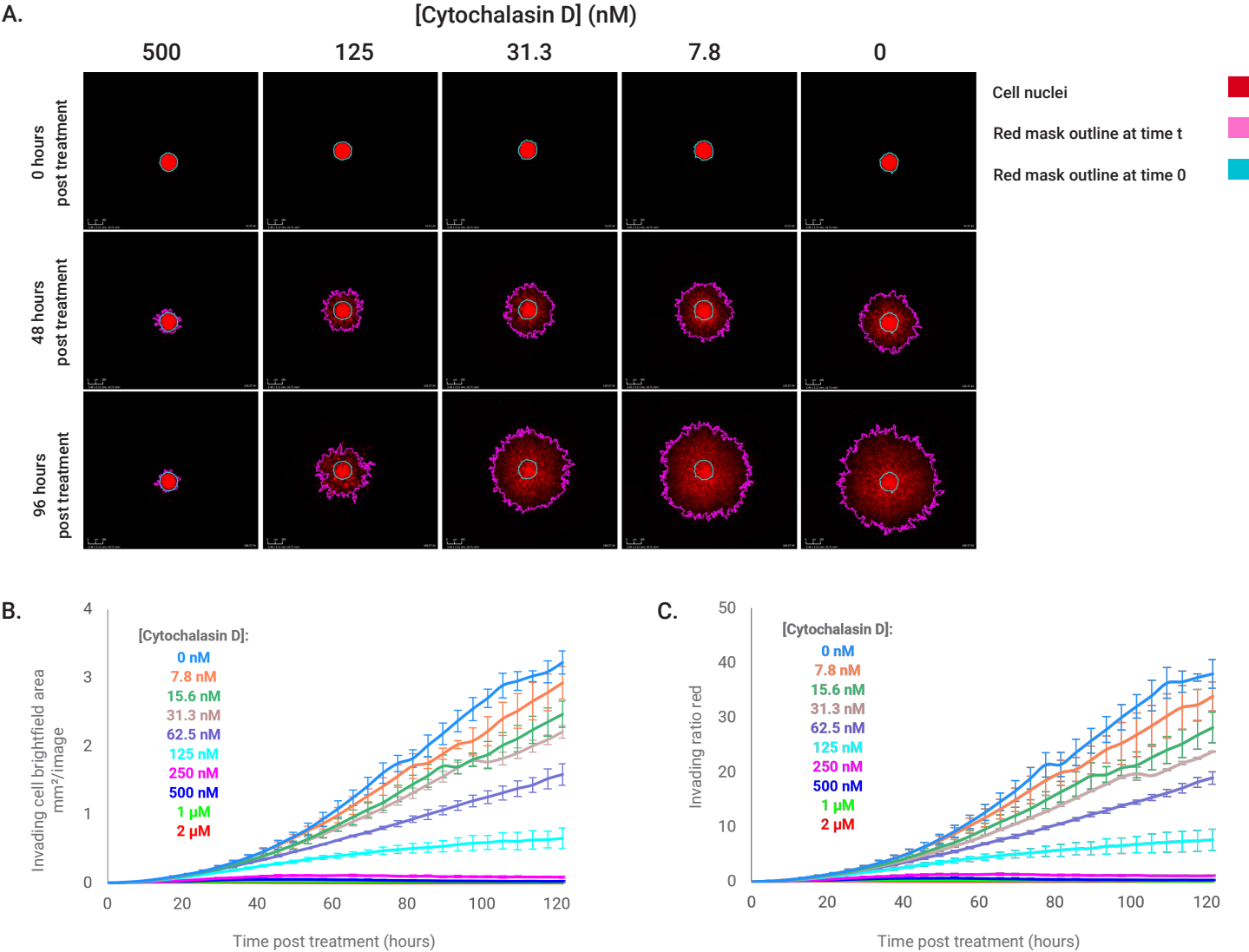
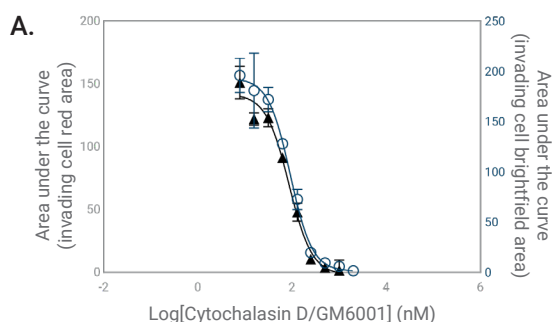


Figure 4. Cytochalasin D dose-dependently inhibits HT-1080 spheroid invasion through red fluorescence recognition. (A) Images show red nuclei of HT-1080 spheroids at 0, 48, and 96 hours after treatment with different concentrations of cytochalasin D. The red total area with cells invading Matrigel was recognized by Agilent eSight software and outlined in pink. For comparison, the red total area outline at time t0 (right after Matrigel and compound addition) was shown in cyan. The impacts of cytochalasin D on the cell invasion progress were quantified by invading cell red area (B) and invading ratio (red) (C) as a function of time.



B.

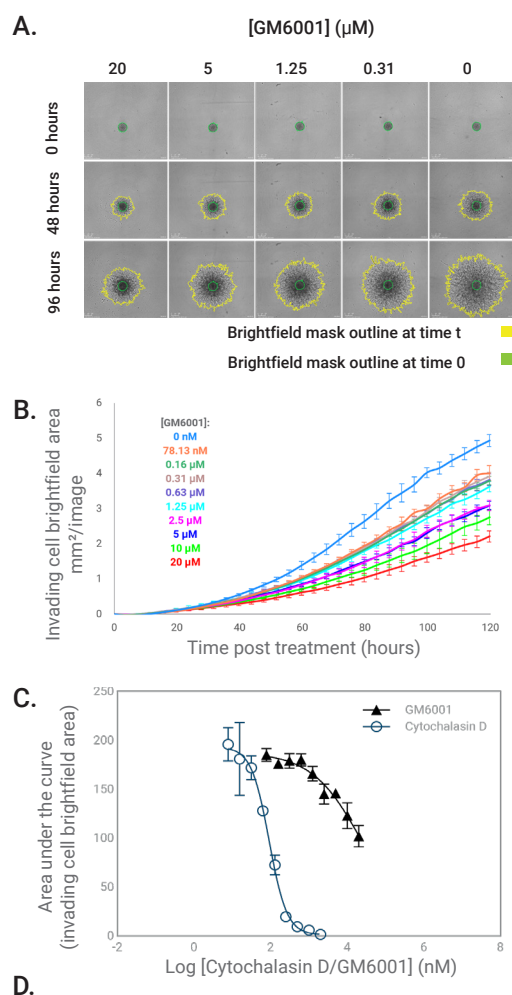
Parameter Analyzed	IC ₅₀ (1 to 120 h)	R ²
Invading cell brightfield area	90.82 nM	0.997
Invading cell red area	84.24 nM	0.988

Figure 5. IC₅₀ calculation based on dose-response curves. (A) Dose-response curves were produced by plotting the area under the curves from the invading cell brightfield area and the invading cell red area as a function of cytochalasin D concentration. (B) The IC₅₀ values were derived from dose-response curves in (A).

These results showed that the eSight 3D spheroid invasion assay can also be conducted label-free (avoiding additional handling of the cells), particularly when there is only one cell type and the invading area can be clearly identified through brightfield imaging. However, when there is more than one cell type being cocultured, or when the invading area cannot be easily identified through brightfield imaging due to impurity interference, the target cell type should be fluorescently labeled. This is recommended as fluorescence parameters may provide more robust results.

The 3D invasion assay can be used to evaluate different drug efficacies

To demonstrate the applicability of this 3D tumor spheroid invasion assay to different anti-invasive compounds, we also treated HT-1080 spheroids with GM6001. GM6001 is a potent, broad-spectrum inhibitor of matrix metalloproteinases (MMP) that inhibits the activity of MMP to degrade the ECM. Figures 6A and B show that GM6001 produces concentration-dependent inhibition of HT-1080 spheroid invasion. The area under the curve of cytochalasin D or GM6001 (0 to 120 hours after drug treatment) was determined as a function of their concentrations, respectively, and plotted in Figure 6C. The inhibitory effect of GM6001 on HT-1080 spheroid invasion was significantly weaker than that of cytochalasin D. The IC₅₀ values based on the brightfield readouts of cytochalasin D or GM6001 inhibiting spheroid invasion were calculated to be 90.82 nM and 26.33 μ M, respectively (Figure 6D).



D.

Parameter Analyzed	IC ₅₀ (1 to 120 h)	R ²
Invading cell brightfield area (GM6001)	26.33 μ M	0.969
Invading cell red area (Cytochalasin D)	90.82 nM	0.997

Figure 6. Analyzing and characterizing GM6001 dose-dependently inhibiting HT-1080 spheroid invasion through brightfield recognition. (A) Images show HT-1080 spheroids at 0, 48, and 96 hours after treatment with different concentrations of GM6001. The whole spheroids with cells invading Matrigel were recognized by Agilent eSight software and outlined in yellow. The spheroid outline at time t₀ (right after Matrigel and compound addition) is shown in green. (B) The invading cell brightfield area was plotted as a function of time. (C) Dose-response curves are produced by plotting the area under the curves from the invading cell brightfield area as a function of cytochalasin D/GM6001 concentration. (D) The IC₅₀ (from 0 to 120 hours posttreatment) values of cytochalasin D/GM6001 were derived from dose-response curves in (C).

Conclusion

Cell invasion is a critical aspect of cancer research in vitro. Intervention in tumor invasion is expected to help limit tumor progression of individuals as tumor invasion is correlated with their metastatic potential. While the wound-healing and trans-well invasion assays give us insight into cell migration and invasion behavior, the 3D spheroid invasion assay is a step further to obtain results closer to the invasion behavior of tumors in vivo. In this application, we combined the in vitro 3D spheroid invasion model with the automatic imaging acquisition and analysis of the Agilent xCELLigence RTCA eSight system to evaluate the invasiveness of HT-1080 spheroids on Matrigel using real time imaging. A comprehensible analysis method was used to quantify cell invasion, which defines the invading cell area as subtracting the total area of the spheroid at time zero (right after the addition of Matrigel and compound) from the total area of the spheroid at a specific time point under control conditions or in the presence of a compound treatment. The availability of metrics and accurate spheroid identification easily enables image-based readouts and analysis to reflect the concentration-dependent influence of cytochalasin D and GM6001 treatment on spheroid infiltration ability.

In conclusion, the xCELLigence RTCA eSight system and its 3D spheroid invasion module can serve as a platform for in vitro analysis of tumor spheroid invasion when tumor cells are cultured alone or cocultured with other cell types, such as fibroblasts or immune cells, facilitating and enhancing the development of new cancer therapies.

References

1. Justus, C. R.; Leffler, N.; Ruiz-Echevarria, M.; Yang, L. V. In vitro cell migration and invasion assays. *JoVE* **2014**, (88), e51046.
2. Zeeshan, R.; Mutahir, Z. Cancer metastasis-tricks of the trade. *BJBMS* **2017**, 17(3), 172.
3. Vollmann-Zwerenz, A.; Leidgens, V.; Feliciello, G.; Klein, C. A.; Hau, P. Tumor cell invasion in glioblastoma. *Int. J. Mol. Sci.* **2020**, 21(6), 1932.
4. Geho, D. H.; Bandle, R. W.; Clair, T.; Liotta, L. A. Physiological mechanisms of tumor-cell invasion and migration. *Physiol. J.* **2005**, 20(3), 194-200.
5. Beaty, B. T.; Condeelis, J. Digging a little deeper: the stages of invadopodium formation and maturation. *Eur. J. Cell Biol.* **2014**, 93(10-12), 438-444.
6. Lim, G. J.; Kang, S. J.; Lee, J. Y. Novel invasion indices quantify the feed-forward facilitation of tumor invasion by macrophages. *Sci. Rep.* **2020**, 10(1), 718.
7. Vinci, M.; Box, C.; Eccles, S. A. Three-dimensional (3D) tumor spheroid invasion assay. *JoVE* **2015**, (99), e52686.